LM-02K093
October 10, 2002

The Effect of pH on Nickel Alloy SCC and Corrosion Performance

D.S. Morton, M. Hansen

02K093

The Effect of pH on Nickel Alloy SCC and Corrosion Performance

D.S. Morton, and M Hansen
Lockheed Martin
P.O. Box 1072
Schenectady, NY 12301

ABSTRACT

Alloy X-750 condition HTH stress corrosion crack growth rate (SCCGR) tests have been conducted at 360°C (680°F) with 50 cc/kg hydrogen as a function of coolant pH. Results indicate no appreciable influence of pH on crack growth in the pH (@ 360°C) range of ~6.2 to 8.7, consistent with previous alloy 600 findings.[1] These intermediate pH results suggest that pH is not a key variable which must be accounted for when modeling pressurized water reactor (PWR) primary water SCC. In this study, however, a nearly three fold reduction in X-750 crack growth rate was observed in reduced pH environments (pH 3.8 through HCl addition and pH 4-5.3 through H_2SO_4 addition). Crack growth rates did not directly correlate with corrosion film thickness. In fact, 10x thicker corrosion films were observed in the reduced pH environments.

INTRODUCTION

The electrochemical environment of a coolant system is primarily characterized by the electrochemical corrosion potential (EcP) and the pH. Subtle changes in EcP (~ 25 mV by coolant hydrogen variation) in proximity to the nickel/nickel oxide phase transition have been shown to significantly affect the crack growth rate performance (up to 7x) of nickel alloys.[2] In contrast, testing of non-sensitized alloy 600 as a function of pH has shown no appreciable influence of pH.[1] The heat treatment that is given to alloy X-750 to generate the HTH condition produces a near continuous chromium carbide coverage that leads to sensitization. Extensive Boiling Water Reactor (BWR) research indicates that the SCC of sensitized materials is more likely dependent upon pH than non-sensitized materials.[3]

This paper reports results from tightly controlled alloy X-750 condition HTH stress corrosion crack growth rate (SCCGR) tests as a function of coolant pH. These tests were conducted to complement the environmental studies of References (1) and (2), such that a complete electrochemical SCCGR dependency can be evaluated for both sensitized and non-sensitized nickel based alloys.

EXPERIMENTAL PROCEDURE

The composition of the alloy X-750 condition HTH heat 84111 material that was employed in this study is provided in Table 1. X-750 HTH grain boundary chromium levels have been measured as low as 6.5 to 8 weight percent. However, chromium depletion measurements are very difficult in X-750 HTH since appreciable precipitate free grain boundary locations are rare.

Table 1: Composition of X-750 HTH Heat 84111 (wt%).

Ni	*Cr*	*Fe*	*C*	*P*	*Mn*	*Si*	*Cu*	*Al*	*Ti*	*B*	*S*
77.43	15.54	7.93	0.04	0.007	0.07	0.05	0.01	0.79	2.60	NR	0.001

The alloy X-750 was fabricated into standard 10.2 mm thick CT specimens. All specimens were fabricated in a longitudinal-transverse (LT) orientation. Test specimens were air fatigue precracked, to a nominal a/W [(1)] of 0.45

[(1)] a is the distance between the crack tip and the load line. W is the distance between the load line and the specimen end (surface in which an unrestrained crack would ultimately intersect).

using the fatigue precracking procedure from ASTM E399 Annex 2. Tests were conducted under pure constant load test conditions at the initial nominal stress intensity factor (K_I) of 51 MPa$\sqrt{m}$.

Constant load SCCGR tests were conducted in active load servoelectric machines with digital control electronics monitored through a computerized data acquisition system. A description of the recirculating high flow rate autoclave system has previously been described.[4] Crack lengths were monitored in-situ using electrical potential drop (EPD) according to ASTM E647, Annex 3, and were verified by post-test destructive examinations (DE). Since alloy X-750 resistivity does not change appreciably with time[5], X-750 EPD resistivity normalization was not performed.

Test Environment

SCCGR tests were conducted in high purity deaerated hydrogenated water (50 cc/kg) at 360°C, with or without dilute additions of either HCl, H_2SO_4, LiOH, or NaOH to vary the coolant pH (pH of 3.8, 4-5.3, 6.2, 8.3 and 8.7 at 360°C). Each test was conducted for 28 days. The test pHs at 360°C (pH_{360C}) were achieved with ~$1.5x10^{-4}$ molal HCl (pH_{360C}=3.8); ~ $5x10^{-6}$ molal H_2SO_4 (pH_{360C} ~4.8); pure deionized (DI) water (pH_{360C} =6.2); ~ $4x10^{-5}$ molal LiOH (pH_{360C} ~8.3); and ~$5.2x10^{-4}$ molal NaOH (pH_{360C} =8.7). The high temperature pH in each test was estimated using the thermodynamic computer code MULTEQ. The version of MULTEQ that was employed had a temperature limitation of 335°C. MULTEQ pH estimates were extrapolated to 360°C through the use of a water dissociation constant which compensates for water density changes.[6] Since H_2SO_4 and HCl effectively dissociate completely, the pH of the these solutions is independent of temperature and is determined simply by balancing hydronium and anion ions for charge neutrality.

Trends in facility pH additive levels were continuously monitored through system in-line conductivity probes and compared with MULTEQ conductivity estimates. Absolute autoclave anion levels were measured by ion chromatography (IC) analysis of autoclave effluent samples. Autoclave cation levels were monitored through analyses of autoclave effluent samples by inductively coupled plasma (ICP) spectroscopy.

RESULTS

Environmental

DI water tests were conducted with extremely high water purity (0.06 µS/cm autoclave inlet and 0.12 µS/cm at the autoclave outlet) since a hydrogen form resin ion exchange column continually polished the autoclave effluent. Consequentially, anion levels were beneath the IC detection limit of ~ 20 ppb. Similarly, cation levels, except for one sample which showed 36 ppb Fe, were below the ICP detection limit of ~10 ppb during the DI water test.

The water conductivity, anion and cation history throughout the tests is provided in Figures 1-3[(2)]. A summary of environmental test conditions is provided in Table 2. These figures illustrate that the coolant chemistry was relatively constant in the HCl and NaOH tests (44 to 26 µS/cm in the HCL test and ~132 µS/cm throughout the NaOH test)[(3)]. In contrast, the coolant chemistry was transient in the H_2SO_4 test. Nine 60 ml 0.01 molar H_2SO_4 additions were made throughout this test (conductivity spikes noted in Figure 2). As illustrated in Figure 2, the conductivity rapidly (40 hours) dropped to ~ 4 µS/cm following each acid addition, presumably due to acid consumption. The autoclave effluent conductivity peak of ~35 µS/cm and low of 2 µS/cm corresponds to pH values of 4 and 5.3, respectively. The pH value of 4.8 (~7.2 µS/cm) was employed for graphical purposes in subsequent figures to represent the pH of the H_2SO_4 test.

The pH additive tests did not use an ion exchange column as is normally employed in typical high purity water tests, since purification would have removed the pH additives. Therefore, some cations (i.e., Si, Ca and Fe) accumulated

---

(2) Conductivity, anion, and cation history results are not available for the LiOH test.

(3) 44 µS/cm HCl corresponds to a pH_{360C} of 4.0 and 132 µS/cm NaOH corresponds to a pH_{360C} of 8.7 via MULTEQ predictions. The measured Cl^- level of 5300 ppb was employed to calculate the reported test pH of 3.8.

to relatively high levels compared with typical high purity water tests (see cation history tables associated with Figures 1-3).

The cation history table associated with these figures illustrates appreciably more dissolved iron in the acid tests compared with the NaOH test. Measured coolant iron and nickel concentrations are semi-quantitatively consistent with MULTEQ and thermodynamic solubility predictions[6] (e.g., at 335°C the iron solubility limit is ~4 ppb at a pH of 6.5, ~1990 ppb at a pH of 4, and ~13 ppb at a pH of 8.5).

Crack Growth Rates

Electrical potential drop (EPD) indicated immediate SCC growth at the start of all tests. Consequently, reported crack growth rates were determined by dividing the actual destructive examination (DE) intergranular SCC extension[(4)] by the test duration. Figure 4 and Table 2 provides summaries of the X-750 crack growth rate measurements as a function of the test pH at 360°C. Included in this table and figure is 360°C pH crack growth rate data at a pH of 6.8 previously reported by our laboratory.[2] This figure illustrates reduced crack growth rates in the two acid tests (~0.3 mils/day) compared with the crack growth rate observed in the other pH tests (~0.8 mils/day) in the pH range of 6.2 to 8.7. As illustrated in Figure 4, actual crack extensions were consistently underpredicted by EPD by a factor of roughly 2. This underprediction occurs consistently for materials with branched crack fronts and results from an uncracked metal ligament conduction path. EPD, however, did well in qualitatively describing the observed pH SCCGR dependency.

Figure 4 illustrates that within the pH range of ~6.2 to 8.7, coolant pH variation did not appreciably influence the crack growth rate of alloy X-750. These results are consistent with alloy 600 SCC results which indicated no significant effects in pH range of 6.9 to 7.4 at 330°C.[1] However, in this study, reduced crack rates were observed in the two acidic X-750 tests.

The observed crack growth rate reduction in reduced pH and sulfur environments was contrary to expectations. In terms of a dissolution SCC mechanism, the solubility of iron and nickel spans ~3 orders of magnitude over the pH range tested, and is higher at low pH. Intuitively, one would expect that crack growth rate would increase when metal solubility limits are high to enhance dissolution. For instance, Andresen concluded that sensitized stainless steel and alloy 600 SCCGR functionality with temperature in aerated high purity water (simulated BWR environment) is consistent with metal oxide solubility behavior (i.e., the maximum SCCGR coincided with the maximum iron solubility limit at the intermediate temperature of ~200°C).[3] Based upon this perspective, SCCGR would have been predicted to be elevated in the pH_{360C} ~4 tests, particularly for alloy X-750 HTH which is sensitized. However, in this study, the lowest SCCGRs were observed in these acid environment tests.

Additionally, reduced crack growth rates at low pH, are not intuitively consistent with a hydrogen assisted cracking mechanism (HAC). In terms of a HAC mechanism, accelerated crack growth was expected in the H_2SO_4 test since sulfur is a known hydrogen recombination poison[(5)].[7] One possible explanation for why a detrimental SCC effect was not observed in the sulfur test is that sulfur never reached the crack tip. Figure 5 provides an optical microscope view of the fracture surface of the H_2SO_4 specimen. This figure illustrates extensive deposition within a narrow region of the specimen precrack. These deposits were identified as Ni_3S_2 by X-ray diffraction analysis. As illustrated in Figure 5, deposits were not present throughout the precrack but rather were concentrated in a precrack region about 30 mil deep starting at the mouth of the precrack. It is speculated that this location was the region in which the concentration of nickel (diffusing from the SCC crack tip) and sulfur (diffusing into the precrack from the coolant) exceeded the solubility limit of Ni_3S_2.

---

(4) The fatigue precrack and SCC crack lengths were measured using an optical microscope, by taking an average of 15 internal points plus the average of two near- side points (as a 16th point).

(5) The presence of a hydrogen recombination poison should give rise to greater metal hydrogen levels which will accelerate SCC if a HAC mechanism is controlling.

Sulfur possibly not reaching the crack tip, however, does not explain the reduction in crack growth rate in the H_2SO_4 test and more interestingly why this reduction was consistent with the reduction observed in the HCl test at a similar pH. The similarity in crack growth rate reduction in these reduced pH tests suggests that the mitigating effect was due to either the pH or a species common in both tests. That is, sulfur or chlorine were not responsible for the reduction in crack growth rate. It is possible because of increased solubility limits in the reduced pH tests that a species common in both the HCL and H_2SO_4 tests caused SCC mitigation. As noted in Figures 1 and 2 elevated levels of Fe, Mn , Mg and Si were common in both acid environment tests. An additional HCl test was conducted with complete purification flow to address this possibility. That is, reduced crack growth rate should not be observed in this test if the SCC mitigation was due to one of the above common species and purification flow prevented coolant impurity buildup. Figure 6 illustrates that a reduced crack growth rate was observed in the complete purification test. Figure 6 also notes that the only species at elevated concentration common with the prior two acid tests was Fe. Since elevated Fe levels were also present in the NaOH which did not show a reduced crack growth rate the most likely explanation for the reduced crack growth rates in the acid environments is an unknown pH effect (e.g., reduced pH is beneficial for crack tip oxide stability, pH changing the EcP, crack blunting?).

Corrosion Measurement

To evaluate if a correlation existed between general corrosion and the observed SCC pH functionality, Electron Spectroscopy Chemical Analysis (ESCA) corrosion measurements were performed on the specimens. ESCA oxide film thickness[(6)] determinations were made on the external surfaces of four alloy X-750 HTH CT specimens tested as part of this study. Figure 7 is a summary of the ESCA corrosion film thickness results.
As illustrated in Figure 7, ESCA average oxide film thickness did not exhibit the same functionality that was observed with SCC with respect to the pH level. The pH 4 oxide film thickness was ten times greater than the pH 8.7 oxide film (14,000 compared to 1300 angstroms), whereas SCC crack growth was ~four times slower under pH 4 test conditions compared to pH 8.7 test conditions.

The lack of a direct correlation between SCC growth rate (SCCGR) and oxide film thickness was also observed in our dissolved hydrogen SCCGR study of X-750 under similar conditions.[2] Figure 8 provides a summary of the Reference (2) SCC and ESCA bulk surface corrosion thickness results as a function of the dissolved hydrogen level. This figure is analogous to Figure 7 (i.e., ESCA oxide film thickness determinations were made on the external surfaces of X-750 HTH CT specimens tested to evaluate SCCGRs). Recent AUGER SCC region oxide film thickness measurements are also presented in this figure. SCC region oxide film thickness measurements were consistent with bulk surface oxide film measurements (i.e., the nitrogen sparge specimen had thicker films than the specimen tested in 149 cc/kg hydrogen). However, analogous to the pH work a correlation between oxide film thickness and SCCGR was not apparent.

It has been suggested[2,4,8] that the influence of many environmental parameters (e.g., dissolved hydrogen, zinc addition) is related not to the extent of corrosion (thickness) but rather to the nature of the oxide films. It has been postulated that the nickel alloy coolant hydrogen functionality[2] correlates with oxide film composition.[8] Specifically, SCCGR is low when either a nickel rich (low hydrogen levels) or chromium rich (high hydrogen levels) oxide film is present and SCCGR is at a maximum when a mixed nickel/chromium rich oxide is formed. Figure 9 illustrates that our coolant hydrogen data[2] is consistent with this observation. However, no correlation was noted between the ESCA determined Ni to Cr ratio and the crack growth rate for the specimens tested as a function of pH, Figure 9.

---

(6) The reported mean oxide film thickness corresponded to the thickness on the depth profile chart where ½ the oxygen is lost between the asymptotic upper and lower limits.

CONCLUSIONS

1. This testing indicates that pH variation in the range of ~6.2 to 8.7 (at temperature) does not significantly influence the crack growth rate of alloy X-750 condition HTH at 360°C, consistent with previous alloy 600 findings.[1] Out of the two primary parameters that typically describe the electrochemical environment of a coolant system (EcP and pH) only EcP (dissolved hydrogen level) appears to be needed to describe nickel alloy SCC under PWR working conditions[9].

2. In this study, a significant crack growth rate reduction (~ 2.8x) was observed in reduced pH tests with two different acids (HCl and H_2SO_4). These results are not intuitively consistent with SCC mechanism expectations. In terms of a dissolution SCC mechanism, the solubility of iron and nickel spans ~3 orders of magnitude over the pH range tested. Intuitively, it would be expected that crack growth rate would be maximized at low pH where higher metal solubility enhances dissolution. In terms of a hydrogen assisted cracking mechanism, accelerated crack growth was expected in the H_2SO_4 test since sulfur is a known hydrogen recombination poison.

3. Alloy X-750 HTH ESCA bulk surface corrosion film thickness did not exhibit the same functionality that was observed with SCC with respect to the pH level. Significantly more bulk surface corrosion occurred in acid environments. An analogous lack of correlation between bulk surface corrosion and SCC was also observed in our recent nickel alloy dissolved hydrogen level SCC crack growth rate study.[2] The dissolved hydrogen level functionality may correlate with the oxide film Ni to Cr composition . The pH SCCGR functionality did not correlate with this quantity.

4. The addition of lithium hydroxide did not accelerate SCC crack growth. In this study X-750 crack growth rate at a pH of 8.3 through LiOH addition was virtually analogous to the crack growth rate at a pH of 8.8 through NaOH addition.

ACKNOWLEDGEMENTS

The following individuals are recognized for their contribution to this effort: Mark Ando and Bill Catlin for their assistance in test design and diligence in test facility operation and Nathan Lewis for his alloy X-750 AEM analyses.

REFERENCES

1. RB Rebak, AR McIlree, ZS Smialowska, "Effects of pH and Stress Intensity on Crack Growth Rate in Alloy 600 in Lithiated+Borated Water at High Temperatures," Fifth International Symposium in Environmental Degradation of Materials in Nuclear Power Systems- Water Reactors, p.511, 1991.
2. DS Morton, SA Attanasio, GA Young, "Primary Water SCC Understanding and Characterization Through Fundamental Testing in the Vicinity of the Nickel/Nickel Oxide Phase Transition," Tenth International Symposium in Environmental Degradation of Materials in Nuclear Power Systems- Water Reactors, 2001.
3. PL Andresen, "Effects of Temperature on Crack Growth Rate in Sensitized Type 304 Stainless Steel and Alloy 600", Corrosion Science Vol. 49, No. 9, p. 714, 9/93.
4. DS Morton, D Gladding, MK Schurman, CD Thompson, "Effect of Soluble Zinc Addition on the SCC Performance of Nickel Alloys in Deaerated Hydrogenated Water," Eighth International Symposium on Environmental Degradation of Materials in Nuclear Power Systems-Water Reactors, p.387, 1997.

5. CD Thompson, DM Carey, NL Perazzo, "Effects of Hydrogen on Electropotential Monitoring of Stress Corrosion Crack Growth," Eighth International Symposium on Environmental Degradation of Materials in Nuclear Power Systems-Water Reactors, p.366, 1997.
6. SE Ziemniak, ME Jones, KES Combs, "Magnetite Solubility and Phase Stability in Alkaline Media at Elevated Temperatures," *Journal of Solution Chemistry*, Vol. 24, No. 9, p. 837, 1995.
7. LA James, "Environmentally-Assisted Cracking of Ferritic Steels in Aqueous Environments; An Interpretative Review," Welding Research Council Bulletin 404, ISN 0043-2326, 8/95.
8. D. Caron, J. Daret, ICG-EAC Meeting, Kyongju Korea, April 23-27, 2001.
9. FJ Pocock, "Water Technology Experience for Materials Protection in Light Water and Heavy Water Reaction Systems" Third International Symposium in Environmental Degradation of Materials in Nuclear Power Systems- Water Reactors, 1987.

Table 2: Test Chemistry and Crack Growth Rate Results

Environment	pH at 360°C	Conductivity (μS/cm)	Initial Stress Intensity Factor (MPa√m)	Average Crack Growth Rate (μm/hr)
$1.5x10^{-4}$ molal HCl without purification flow	3.8	44 to 26	50.8	0.24
$5x10^{-6}$ molal H_2SO_4 without purification flow	4-5.3	2 to 34	50.7	0.30
DI water with complete purification flow	6.2	0.1	51.1	0.78
$5.2x10^{-4}$ molal NaOH without purification flow	8.7	132	51.3	0.90
~$4x10^{-5}$ molal LiOH with complete purification flow	8.3	~34	50.1	0.87
$1.02x10^{-4}$ molal HCl with complete purification flow	4.0	32 to 34	51.1	0.42

Figure 1: X-750 360°C HCl (pH~3.8) Test Chemistry

(ppb)

Point	Cl	Ca	Fe	Mg	Mn	Ni	Si	Zn
1	5,300	70	880	180	480	28	190	51
2	5,300	250	590	240	520	49	400	28

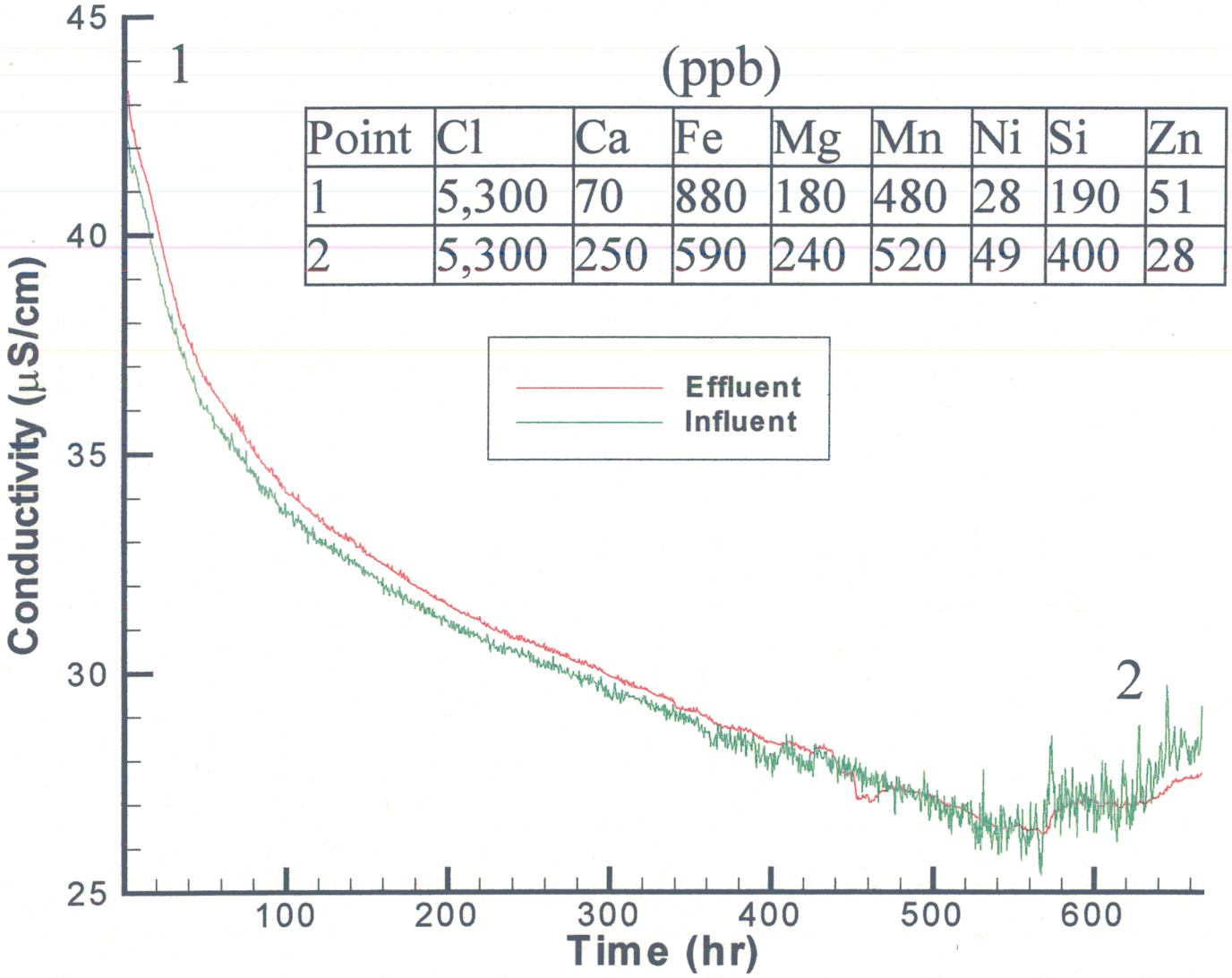

Figure 2: X-750 360°C H_2SO_4 (pH~4 to 5.3) Test Chemistry

(ppb)

Point	SO_4	Ca	Fe	Mg	Mn	Ni	Si	Zn
1	1000							
2	1880	19	290	84	51	<10	170	<3
3	760	47	140	140	44	<10	750	<3

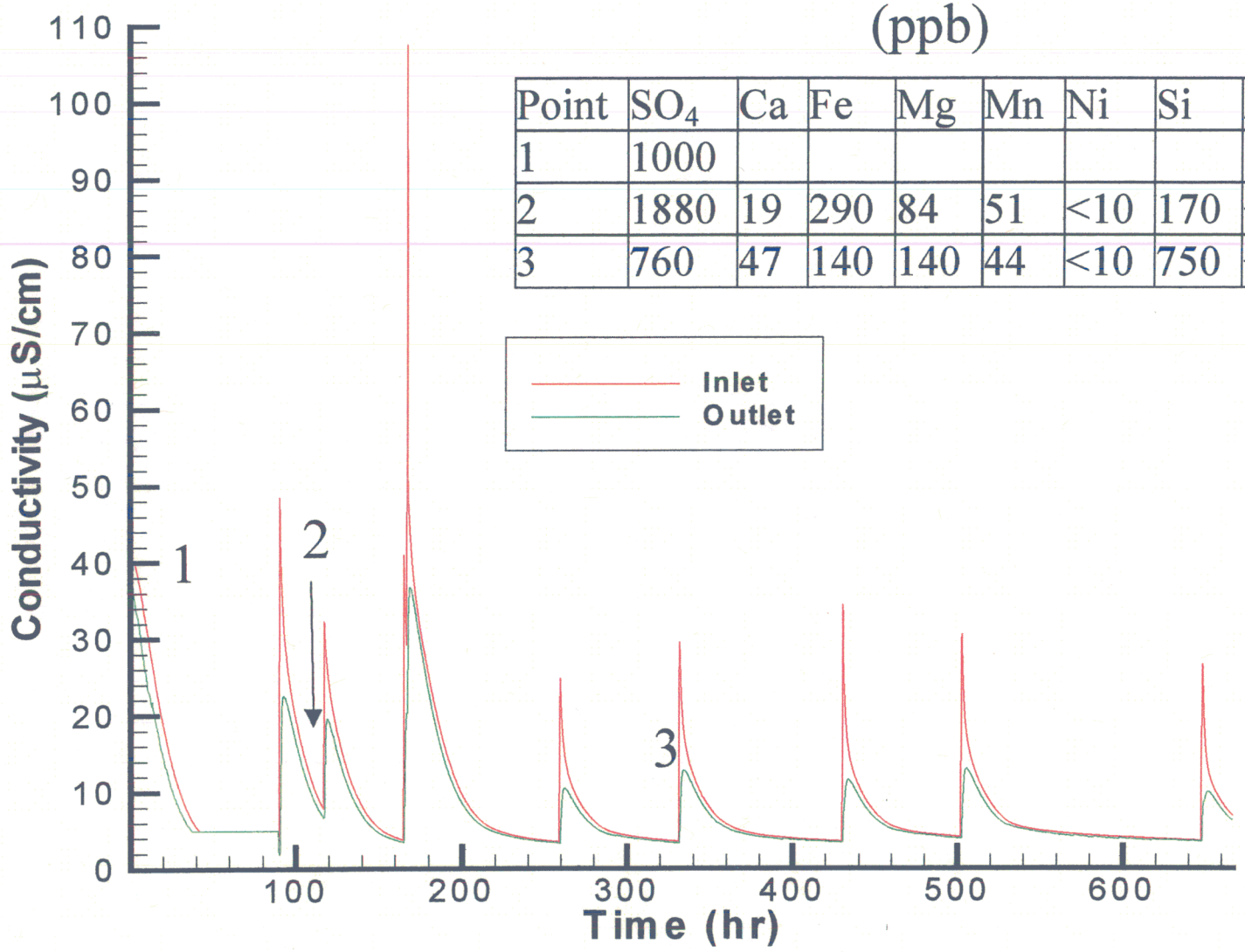

Figure 3: X-750 360°C NaOH (pH~8.7) Test Chemistry

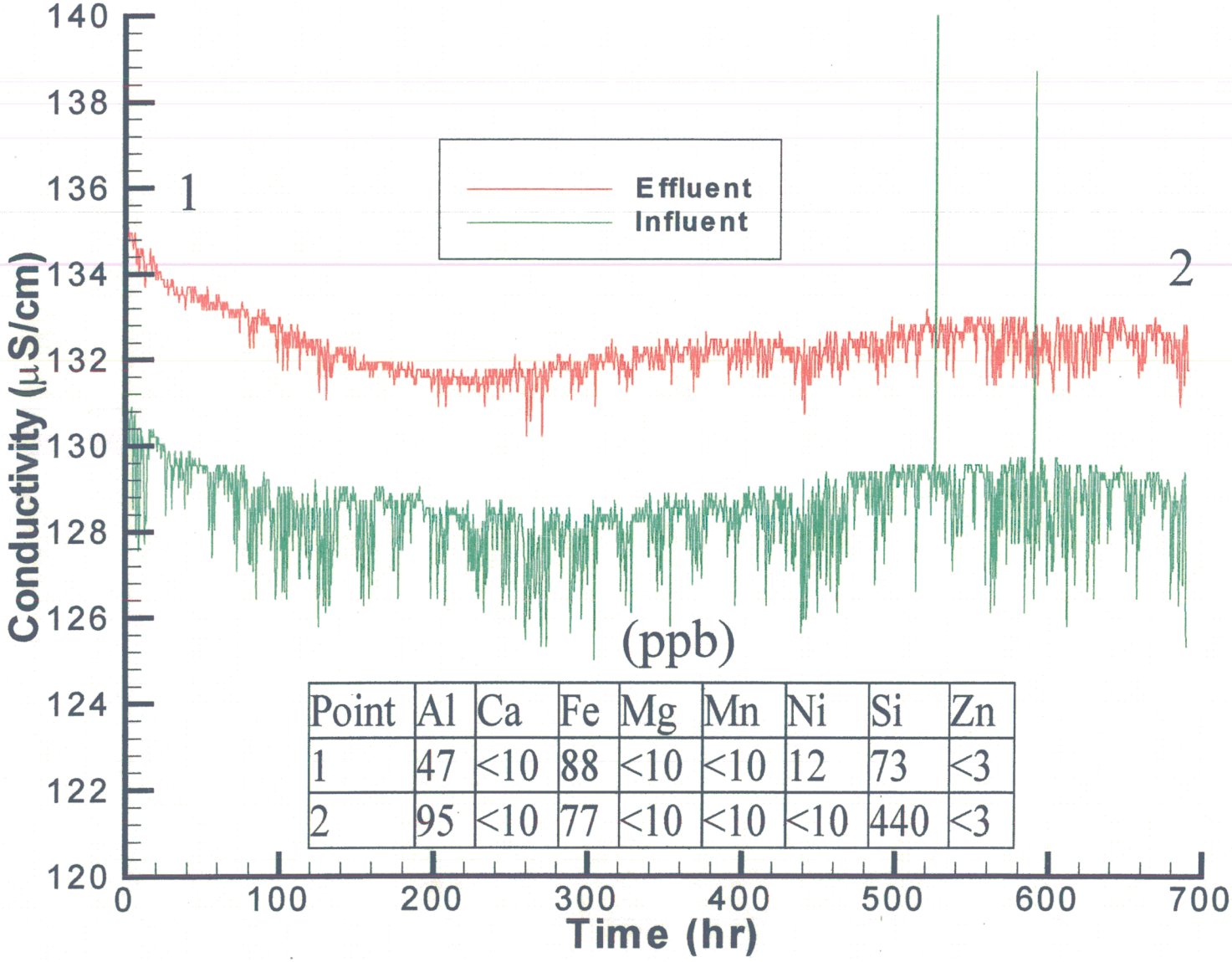

(ppb)

Point	Al	Ca	Fe	Mg	Mn	Ni	Si	Zn
1	47	<10	88	<10	<10	12	73	<3
2	95	<10	77	<10	<10	<10	440	<3

Figure 4: Comparison Between Actual and EPD SCCGR vs. pH

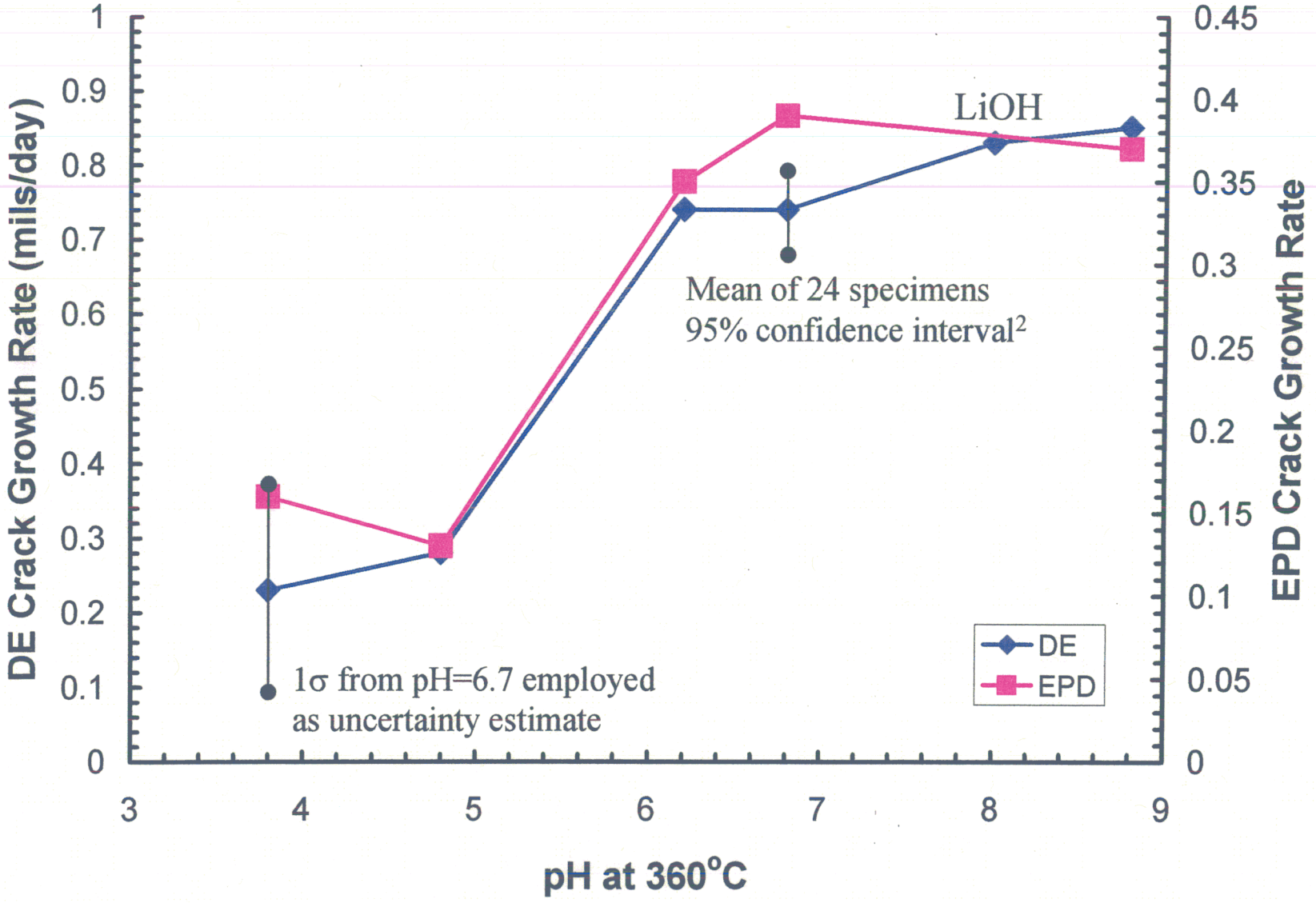

Figure 5: Ni_3S_2 Deposits Observed Only in an ~30 mil Region of the Precrack (X-750 360°C H_2SO_4 Test)

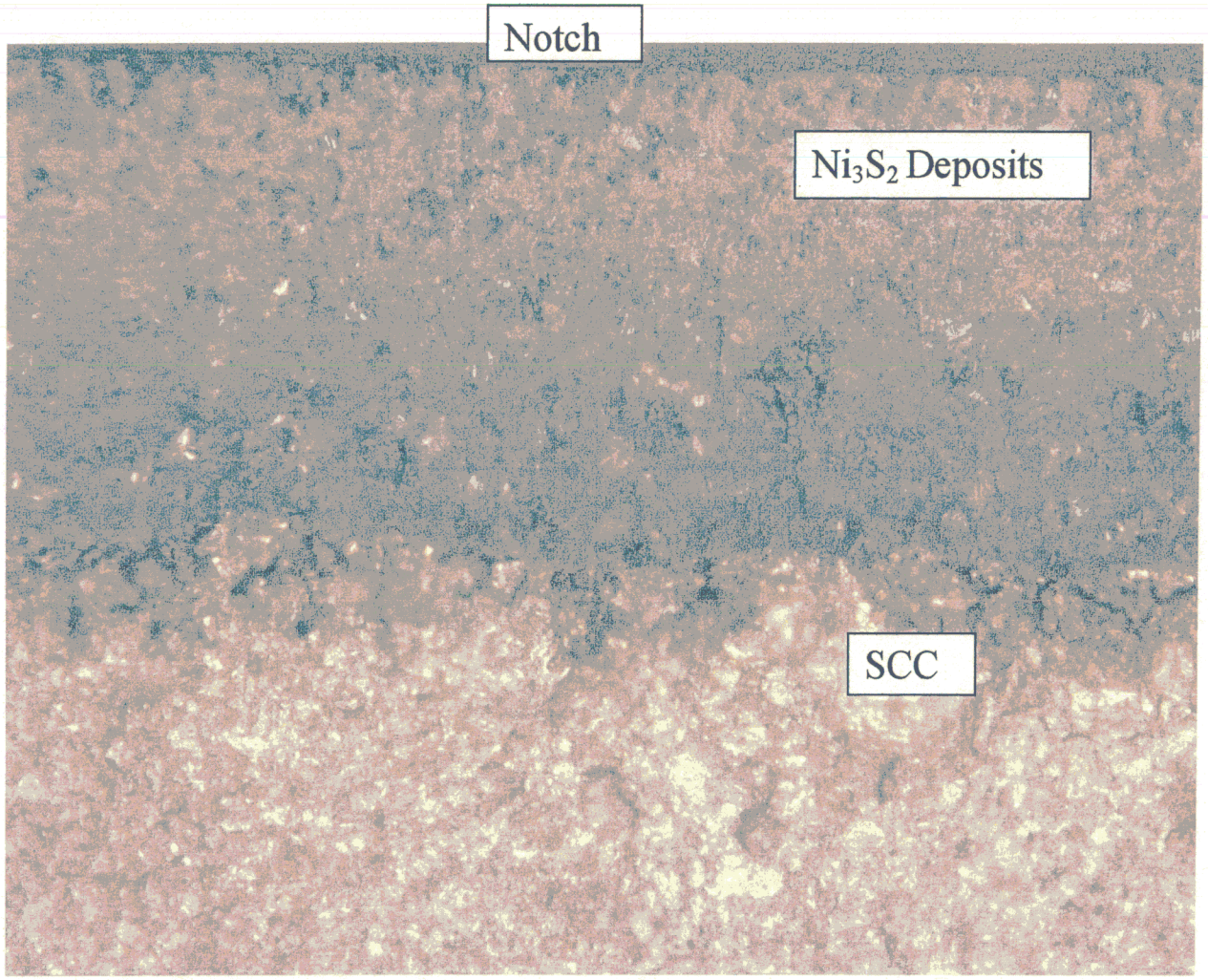

Figure 6: X-750 360°C HCl (pH~4) Complete Purification Column Flow Test Results

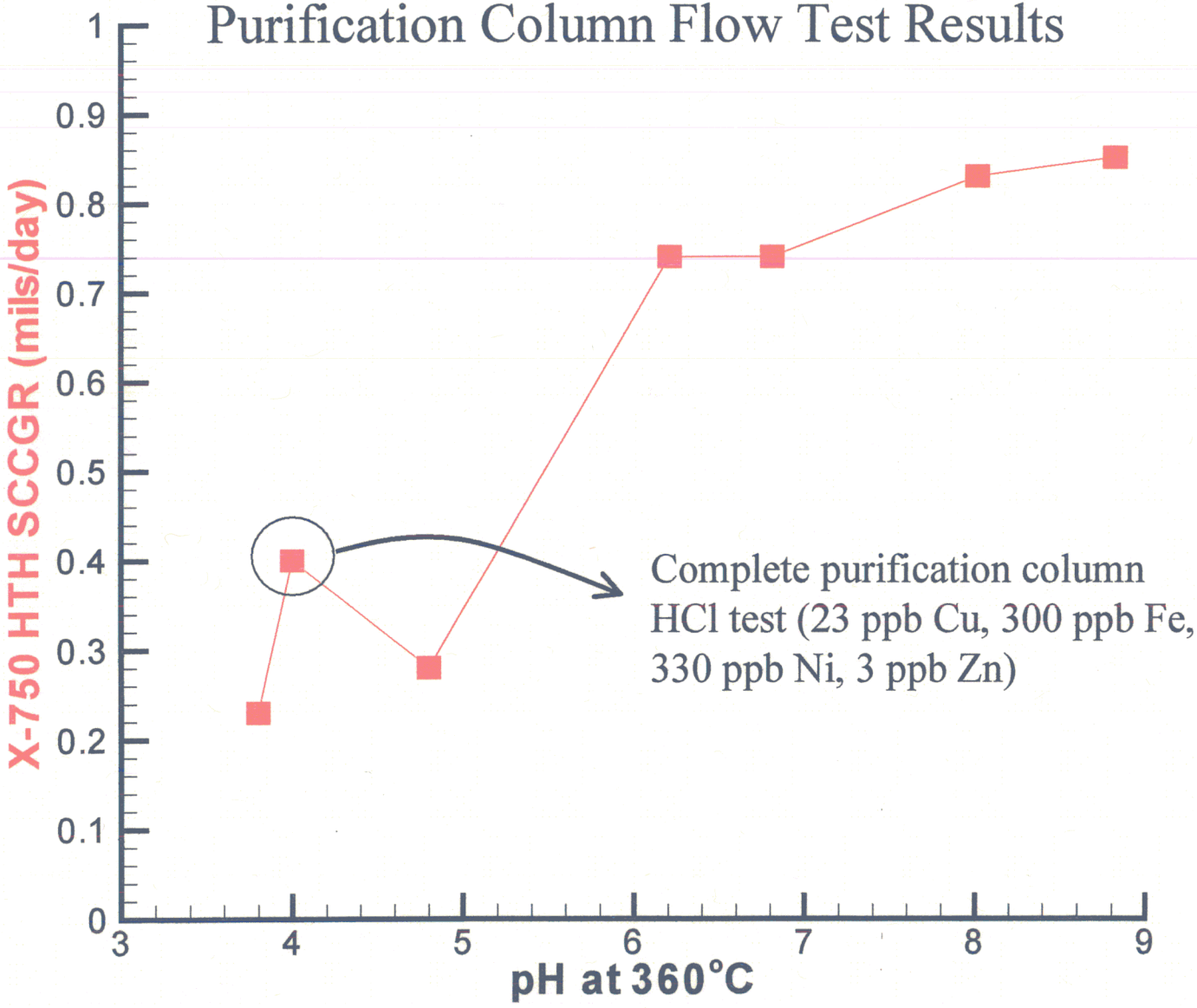

Figure 7: Comparison between SCCGR and Bulk Surface Corrosion Thickness as a Function of pH

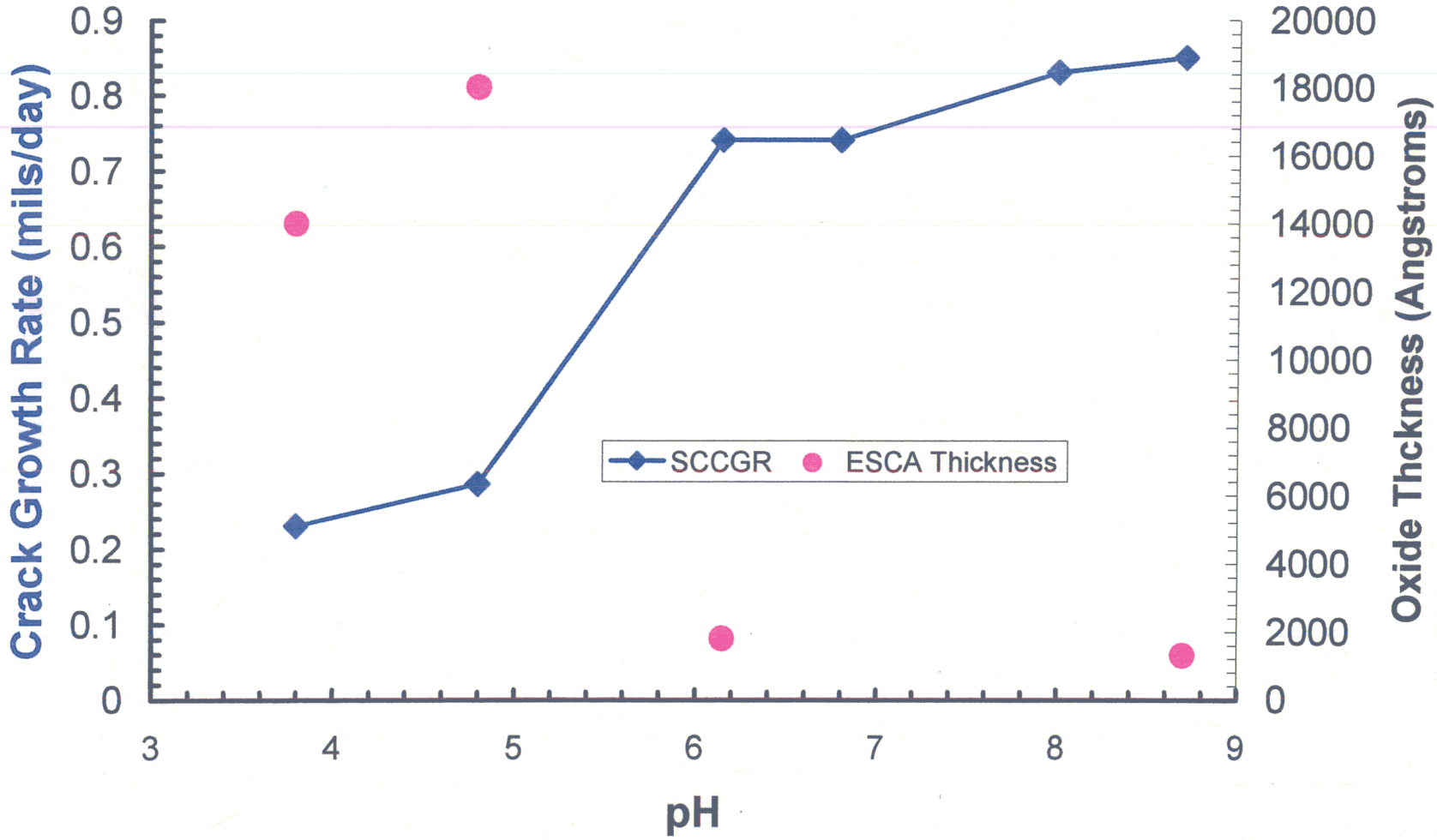

14

Figure 8: Comparison between SCCGR and Bulk/SCC Corrosion Thickness as a Function of Dissolved Hydrogen Level[2]

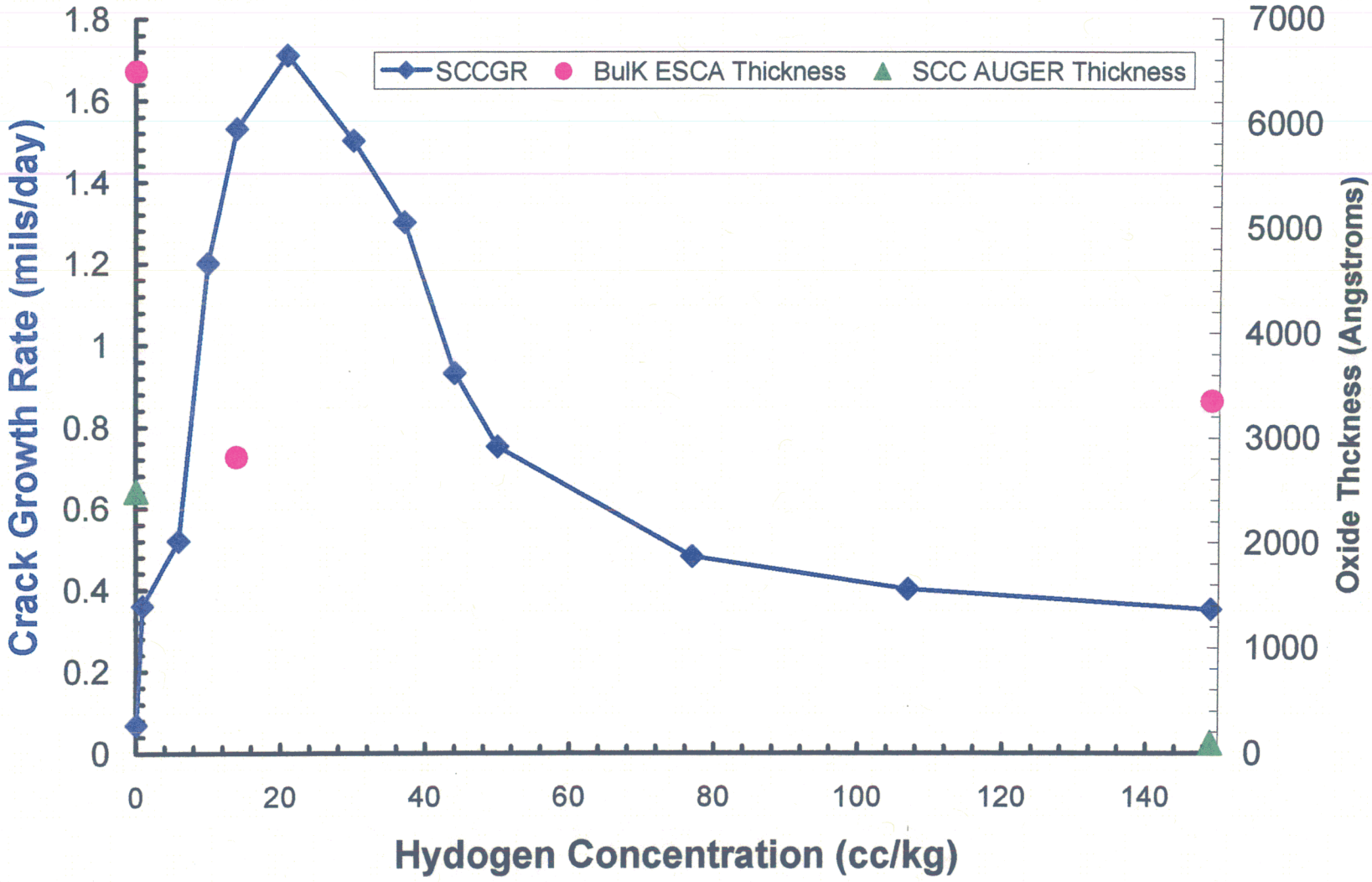

91

Figure 9: No Correlation between SCCGR and Ni/Cr Ratios Observed in Bulk Surface Corrosion Oxides Test as a Function of pH and Dissolved Hydrogen Level[2]